

Thermal Stresses in Butt-Jointed Thick Plates from Different Materials

Photothermoelastic models were used to investigate the formation of thermal stress concentrations

BY Z. ABDULALIYEV, S. ATAOLU, AND D. GUNAY

ABSTRACT. A variety of materials are used as elements and constructions in many branches of industry. These materials are exposed to heavy variable mechanical and thermal loads during service. The resultant stresses of variable thermal and mechanical loads are added and they may reach high levels in the stress concentration regions of the elements, leading to the formation of cracks. In this study, the formation of thermal stress concentrations was investigated using photothermoelastic models for butt-jointed thick plates from different materials at the weld zone. In the models, the effect of the slope of the materials' connection plane with respect to the normal plane of the plate on the stress distribution was studied. In the stress concentration regions of the considered joints, the effect of the different geometric factors was also investigated on the models in order to arrange the concentration of the thermal stresses as required.

Introduction

Many constructions, widely used in engineering and other sectors, are made of different materials using welding. Temperature changes during the working process result in thermal stresses in the welding region of the different materials. These thermal stresses reach high magnitudes and vary with high gradients (Refs. 1–6). These stresses can combine with the stresses from the other variable mechanical loads acting on the elements of the constructions. Thus, they can lead to the formation of cracks due to the variation of all those stresses in the welding region. Value and distribution of the thermal stresses are affected in the connected region of different materials by the slope and location of the contact plane. Investi-

gation of thermal stresses in the associated regions can provide important information for the optimum design of the welding region. Depending on the information obtained from this kind of research, the slope angle of the contact plane of the different materials and the optimum geometry of the welding region in the design can be modified.

Elliott and Fessler (Ref. 7) measured the elastic, elastic-plastic, and residual plastic strains in the surfaces of sections of weldments using photoelastic coatings and Moiré interferometry. The effect of the slope of the joint plane on thermal stress distribution is an important subject for the strength of the construction, as is optimum design of the region. In this study, thermal stresses due to uniform temperature changes, which form in thick butt-joint-welded plates from different materials, are examined by the photothermoelastic method (Refs. 8, 9). The effects of some geometric factors and slope of the connection plane with respect to the plates' normal plane on value and distribution of the thermal stresses were also investigated. In the jointed constructions, the thermal stress distribution for the single-V weld joint could be obtained by superimposing the results of the experiments. The following assumptions are valid in the tests:

- The plates of different materials are jointed with each other on a plane;
- No variation in the material properties due to temperature in the process of welding;
- The residual stresses due to the welding process aren't taken into account;
- Reinforcement and throat are in the same plane with those of jointed plates.

Analysis Technique of the Models

In order to model thermal stresses in the joint regions of the different materials, the mechanical modeling method of photothermoelasticity is employed because of its precision and availability of easy application (Refs. 5, 6, 8, 9). Mechanical modeling of thermal stresses is based on the freezing/unfreezing property of strains of some optically sensitive materials. Mechanical modeling of thermal stresses as known is summarized below (Refs. 5, 6, 8, 9).

A geometric simulation factor is set up to measure the stresses accurately in the concentration regions of the structure. It is assumed that the structure is divided into "i" number of free elements with uniform thermal expansion, depending on the material characteristics, geometry, and gradient of the temperature distribution. The free thermal expansion, ϵ_i , of the elements is calculated as follows:

$$\epsilon_i = \alpha_i \Delta T_i \quad (1)$$

where α_i is the thermal expansion coefficient and ΔT_i represents the increment of the temperature of the relevant elements, respectively. The model of the structure is constructed from the parts associated with the elements of the structure mentioned previously. The modeling scale of the free thermal expansions κ , is chosen as $\kappa = [(\epsilon_i)_n / (\epsilon_i)_m]$, where $(\epsilon_i)_n$ denotes the free thermal expansion of the element of the structure and $(\epsilon_i)_m$ is the uniform strain that will be frozen by a mechanical load in the relevant part of the related model. The uniform strains, which are equal to the strains in the related parts of the model, $(\epsilon_i)_m$, are formed in the samples via the mechanical loads, and then they are frozen under the proper loads in the relevant samples. The parts of the model are cut out from the uniform deformation regions of the relevant samples. The parts are glued together with a special adhesive along the required surfaces. The prepared model is heated to its critical temperature in the oven. The strains, which earlier had

KEYWORDS

Thermal Stresses
Joint Materials
Photothermoelasticity
Joint Design

Z. ABDULALIYEV is with Metallurgical and Materials Engineering Dept., Faculty of Chemical and Metallurgical Engineering, Istanbul Technical University, Istanbul, Turkey. S. ATAOLU and D. GUNAY are with Div. of Mechanics, Civil Engineering Dept., Faculty of Civil Engineering, Istanbul Technical University, Istanbul, Turkey.

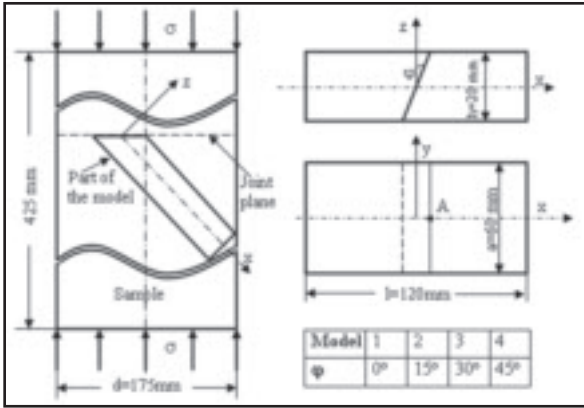


Fig. 1 — Schemes of models and samples used in the experiments.

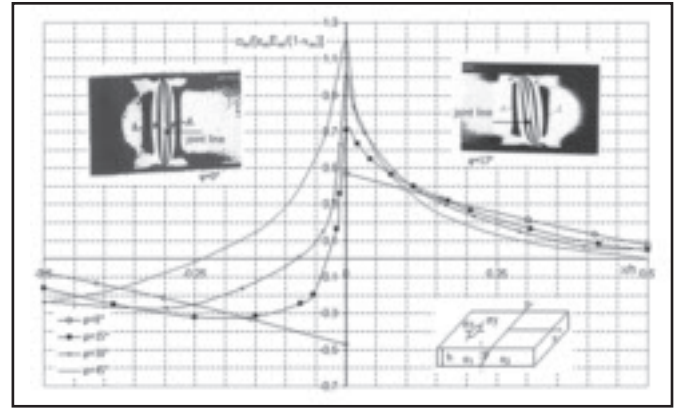


Fig. 2 — Variations of dimensionless stress component, σ_x , on the free surface for the model of joints for different bevel angles with the photos of isochromatic patterns.

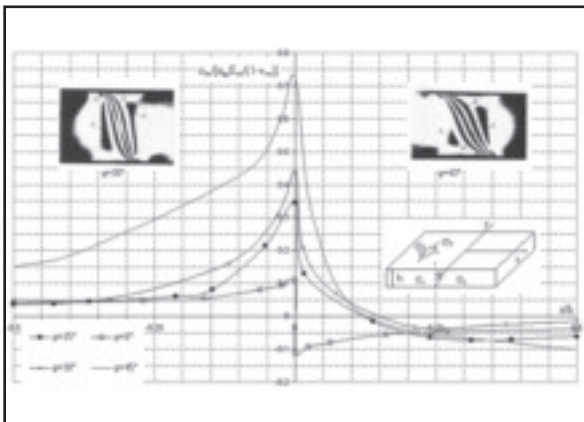


Fig. 3 — Variations of dimensionless stress component, σ_y , on the free surface for the model of joints for different bevel angles with the photos of isochromatic patterns.

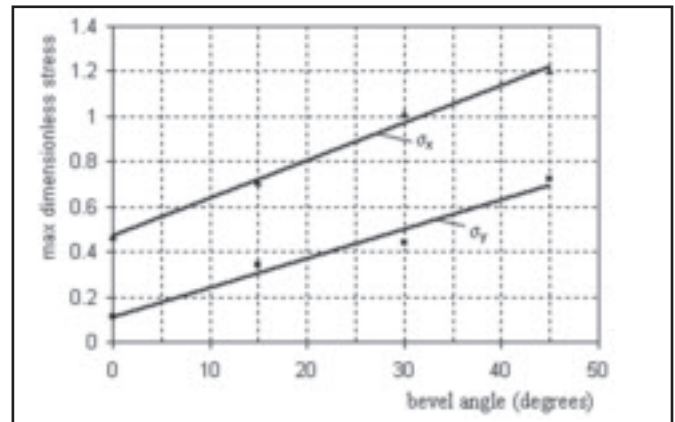


Fig. 4 — Variation of the maximum dimensionless thermal stress components, σ_x and σ_y , on the free surface vs. the bevel angle.

been frozen in the parts, are unfrozen and the stress state associated with the thermal stresses to be examined in the structure is formed in the model. The model is cooled to room temperature. The stress-strain state of the model is frozen in this way. The stress state of the model is researched using photoelasticity techniques (Refs. 10, 11). The actual stresses in the structure, σ_n , are calculated by the stresses obtained in the model, σ_m , using the following formula:

$$\sigma_n = \frac{1 - \nu_m E_n}{1 - \nu_n E_m} \kappa \sigma_m \quad (2)$$

where ν represents the Poisson's ratio and E is the modulus of elasticity of the materials. Indexes m and n refer to the model and the actual structure, respectively.

In this study, the mechanical modeling method is applied in order to investigate the thermal stresses of the butt-joint-welded thick plates made of the materials in the uniform temperature change, which differ from each other with the value of

the thermal expansion coefficients. The effect of the different bevel angles in joints on stress distribution and some different geometric factors to reduce the stress magnitude in the region of the interface were investigated.

Preparation of the Model of the Butt-Joint-Welded Thick Plates

It is assumed that the thermal expansion coefficients of the materials of these welded plates are α_1 and α_2 , respectively. Thermal stresses due to uniform temperature changes, ΔT , in the examined butt-jointed plates are proportional to the difference of free thermal expansion $[(\alpha_2 - \alpha_1)\Delta T]_n$ of the welded materials. As understood, the model can be constructed in two parts and to form is enough uniform strain associated with the difference obtained above in a part of the model. This uniform strain is computed as $\epsilon_{rm} = \epsilon_{\theta m} = 0.015$ using the modeling scale of the free thermal expansion, κ . The calculated expansion must be formed and frozen in a sample, taking into account the modeling

scale of the free thermal expansion, κ , for preparing the model. The expansions are formed by axial compression and frozen in long cylindrical samples prepared from an optic-sensitive material based on epoxy resin. A model part is cut out from the uniformly deformed center region of the sample. The plane of the part, which will be glued with another part, must coincide with the cross section of the sample as shown in Fig. 1. The other part of the model is made of the same material without any prestraining applications. Two parts are glued together with epoxy resin-based cement. The final shape and dimensions of the model are formed by machine tools.

In the experiments, the angle between the interface and the normal of the plate plane, represented by φ , is varied as 0, 15, 30, and 45 deg, and the thermal stresses are investigated for each joint. Optically sensitive material-based epoxy resin, free from residual stress, which is employed for the models, has the characteristics at its own critical temperature of 150°C, as follows:

Elastic modulus, $E_m = 21$ MPa, fringe-

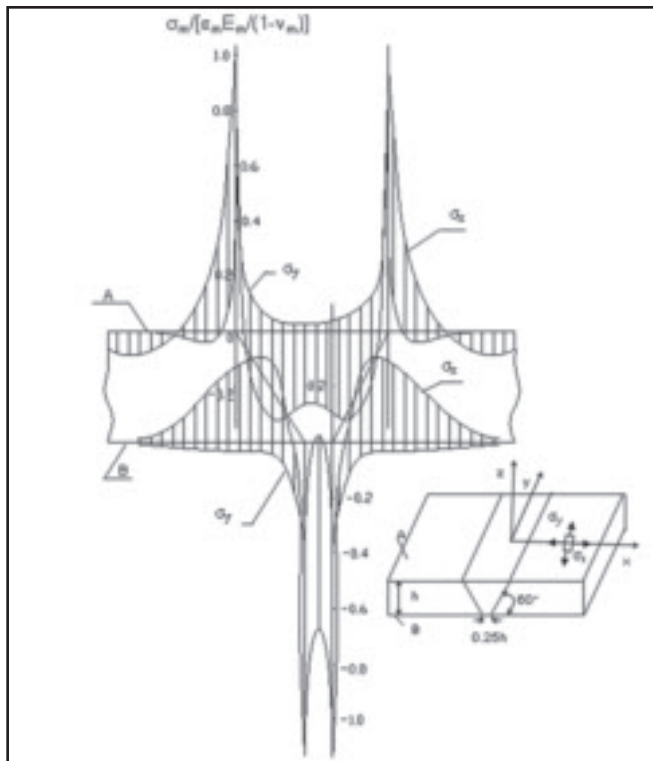


Fig. 5 — Distribution of stress components in a single-V weld joint with bevel angle $\varphi = 30$ deg.

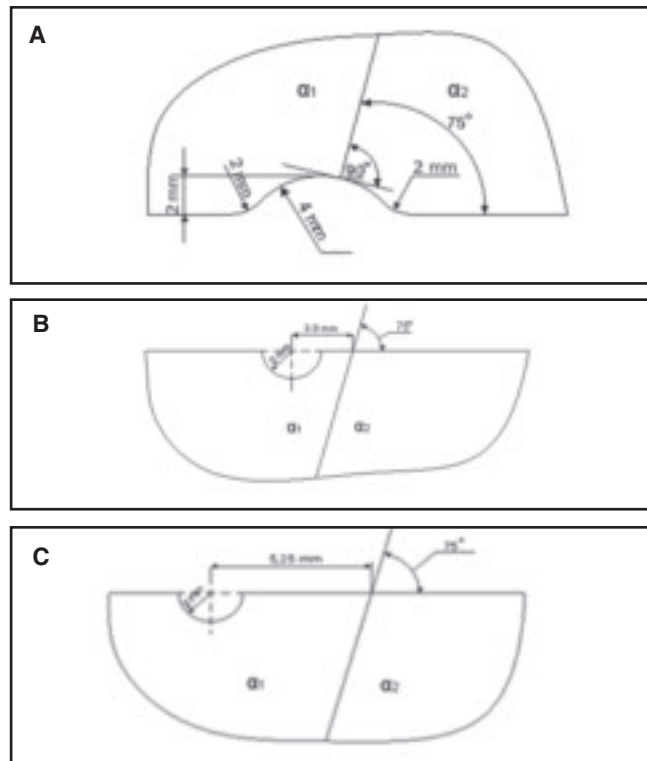


Fig. 6 — The examined geometric factors for the effect on the concentration of thermal stress components on the joint region. A — Changing bevel angle by the help of a cylindrical surface; B — the cylindrical cavity is located 3.90 mm away from the connection line; C — the cylindrical cavity is located 5.25 mm away from the connection line.

stress value, $\sigma_0^{1.0} = 0.365$ N/(cmxfringe) and Poisson's ratio $\nu_m \cong 0.5$.

Stress State Analysis of the Models

It is enough to investigate the stresses acting on the symmetry plane, xOz , in the tested models since this section is related to the diametrical plane of the constructions having relatively big diameters. Stress distribution of the models on the symmetry plane is only related to the plate's thickness h , because the mentioned plane is far away from free lateral planes. Therefore, distributions of dimensionless stress components, $\sigma_m/[E_m \varepsilon_m/(1-\nu_m)]$, in this region on dimensionless coordinates, x/h and z/h , don't depend on the h value. On the symmetrical planes of the tested models, the photographs of isochromatic patterns, characterizing the distributions of the thermal stress, are given with variations of dimensionless stress components σ_x and σ_y vs. x/h on the surface ($z = h/2$ plane) in Figs. 2 and 3. The stress distribution is skew-symmetric on the ($\pm h/2$) surfaces of the examined jointed plates. Therefore, the graphs of stresses are given only in surface ($z = h/2$). It is apparent from Figs. 2 and 3 that distributions of di-

mensionless thermal stress components σ_x and σ_y , around the interface are local and include the region, which approximately is a distance, h , away from the interface. When the bevel angle of joint, φ , is 0 deg, dimensionless stress component, σ_x , increases with the high gradient while approaching the contact line of the materials and reaches the value of ± 0.47 as shown in Fig. 2. Here, the value of dimensionless stress component, σ_x , which is calculated by a numerical method, is equal to ± 0.5 (Ref. 12). The obtained results show that values of the thermal stress components increase in the joint region when the bevel angle is getting greater, for instance, ± 1.2 for 45 deg, but their gradients decrease in that region as shown in Figs. 2 and 3.

The skew-symmetric property of mentioned stress on the examined joints is used for evaluating the time-edge effect (Refs. 10, 11) of the model material to its stress distribution. It is noted that this is done taking the mean value acting stresses on the relevant point of the surfaces, $z = \pm h/2$, for every joint.

Graphs of variations of the max dimensionless thermal stress components, σ_x and σ_y , vs. slope angle of the interface in the connection zone of the different materials around the point A (see Fig. 1) are shown in Fig. 4. According to Fig. 4, variation of the

maximum dimensionless stress components vs. bevel angle can be considered as linear.

The results obtained in the model where the slope angle of the interface is 30 deg are used in order to evaluate the thermal stress components in a single-V weld joint by the superposition method — Fig. 5.

The aforesaid statement in the experiments can be exemplified by assuming a couple of stainless steel-carbon steel materials. If the maximum stress is computed at the joint of the couple by a bevel of 45 deg for $\Delta T = 200^\circ\text{C}$ of the structure, using Equation 2 with constants as follows:

$$\begin{aligned} \alpha_{\text{steel}} &= 12 \cdot 10^{-6} \text{ } 1/^\circ\text{C}, \\ \alpha_{\text{stainlesssteel}} &= 16 \cdot 10^{-6} \text{ } 1/^\circ\text{C}, \\ E_{\text{steel}} &= E_{\text{stainlesssteel}} = 200 \text{ GPa, and} \\ \nu &\cong 0.3 \text{ (Ref. 4).} \end{aligned}$$

The results obtained of σ_x and σ_y for the structure are 274 and 168 MPa, respectively.

It can be concluded that the thermal stress components in combination with stresses from other loads and defects due to the joining technology could cause crack generation in the joint region of the constructions.

Different methods of reducing the thermal stress level in the connection zone of different materials were investigated. In this way, the effect of some geometrical factors on the concentration of thermal

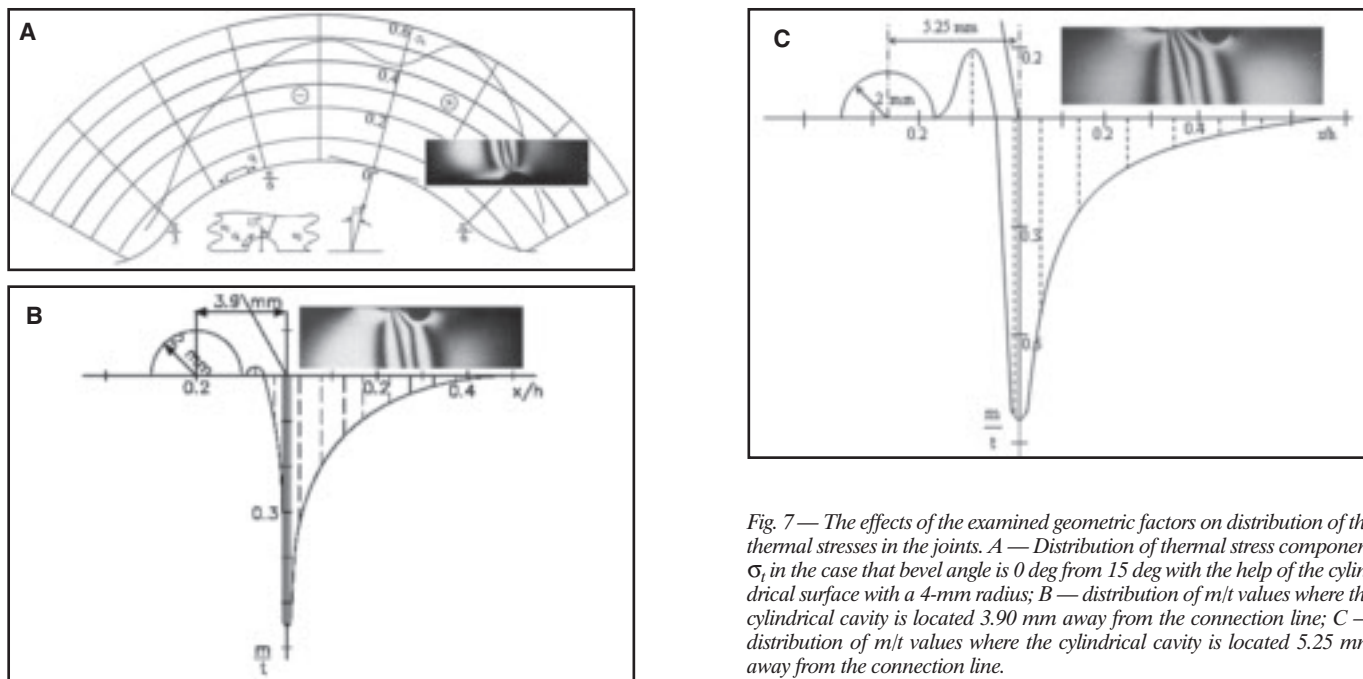


Fig. 7 — The effects of the examined geometric factors on distribution of the thermal stresses in the joints. A — Distribution of thermal stress component σ_r in the case that bevel angle is 0 deg from 15 deg with the help of the cylindrical surface with a 4-mm radius; B — distribution of m/t values where the cylindrical cavity is located 3.90 mm away from the connection line; C — distribution of m/t values where the cylindrical cavity is located 5.25 mm away from the connection line.

stress components was also investigated around the contact line on the free surface — Fig. 6A–C. As an example, mentioned factors are examined in the joint where the slope angle is 15 deg. The slope angle of the interface near the free surface of the joint was changed from 15 to 0 deg using a cylinder surface whose radius is 4 mm and the axis is parallel to y-axis (Figs. 1, 6A) was considered for this case. The max dimensionless stress component, σ_r , around the contact point (Fig. 7A) corresponds to the value of $\varphi = 0$ deg — Fig. 2. It is seen from Figs. 2 and 7A that dimensionless stress value decreases from 0.7 to approximately 0.42.

The effect of the cylindrical cavities at the free surface of the joints, made parallel to the contact line and also at different distances from the line (Fig. 6B, C), are investigated in two different models. Photographs of isochromatic patterns, characterizing the effect of the cylindrical cavities on the thermal stress distribution, are shown in Fig. 7B and C, respectively. These effects can be evaluated by comparing the changes in the relevant m/t graphs for the models, where m is the fringe order and t is the thickness of the slice on the measured points. In comparison, the smaller the distance, the lower the value of the stress components at the contact line. Thus, as the distance decreases by 25%, the maximum value of m/t decreases by approximately 23%.

Conclusions and Discussions

It is important to compute values of

local thermal stresses in the weld region for jointed constructions such as pressure vessels applied in nuclear power plants, the chemical industry, etc. In this study, mechanical modeling of thermal stresses was used to investigate the concentration of thermal stress components in butt joints in thick plates and the effect of variation of the bevel angle value on the stress distribution in joints. The following assumptions were made in the experiments for simplification:

- Materials are continuous in the welding zone;
- The plates of different materials are jointed with a plane;
- Reinforcement and throat, which occur during the welding process, are in the same plane with those of jointed plates;
- No variation in the material properties and toe and underbead cracks due to temperature in the process of welding;
- The residual stresses due to the welding process aren't taken into account in the joint, and can be investigated with some specific methods.

The following was observed:

1. Thermal stress components around the contact line on the free surfaces of the jointed plates increase with the increase in the bevel angle, but the gradients decrease.

2. There is a relationship between the bevel angle and the maximum thermal stress components on the free surfaces just near the contact line, which can be considered as linear.

3. The maximum values of thermal stress components around the contact line on the

free surface of the joint can be regulated by applying some design proposals based on the experiments presented herein.

References

1. Boley, A. B., and Weiner, J. H. 1960. *Theory of Thermal Stresses*. New York, N.Y.: Wiley.
2. Nowacki, W. 1986. *Thermoelasticity*. New York, N.Y.: Pergamon Press.
3. Noda, N., Hetnarski, R. B., and Tanigawa, Y. 2003. *Thermal Stresses*. New York, N.Y.: Taylor & Francis.
4. Melan, E., and Parkus, H. 1953. *Wärmespannungen Infolge Stationärer Temperaturfelder*. Vienna, Austria: Springer.
5. Abdulaliyev, Z., Egrican, N., and Karadag, V. 2000. Three dimensional photoelasticity modeling of thermal stresses in cylindrical structures. ASME ETCE New Orleans, La.
6. Abdulaliyev, Z., and Karadag, V. 2002. Analytical and experimental analysis of thermal stresses around semicircular fiber inclusions plate with different materials. ASME ESDA Istanbul, Turkey.
7. Elliott, K. S., and Fessler, H. 1996. Elastic-plastic strain distributions at fillet welds. *J. Strain Anal. Eng. Design* 31(3): 215-s to 230-s.
8. Leven, M. M., and Sampson, R. C. 1959. Photoelastic stress and deformation analysis of nuclear reactor components. *Proc. Soc. ESA* 17(1).
9. Slot, T. 1965. Photoelastic simulation of thermal stresses by mechanical prestraining. *Proc. Soc. Exp. Stress Anal.* 22 (2).
10. Frocht, M. M. 1941. *Photoelasticity*, Vol. 1. New York, N.Y.: Wiley.
11. Kuske, A., and Robertson, G. 1974. *Photoelastic Stress Analysis*. New York, N.Y.: Wiley.
12. Horvay, G. 1954. Thermal stresses in rectangular strips. *Proc. II. National Cong. of Appl. Mech.*, ASME, New York, N.Y.